

Properties of multiqubit variational quantum states representing weighted graphs and their computing with quantum programming

Kh. P. Gnatenko ^{1,2}, A. Kaczmarek ²

¹*Ivan Franko National University of Lviv,
Professor Ivan Vakarchuk Department for Theoretical Physics,
12 Drahomanov St., Lviv, 79005, Ukraine*

²*SoftServe Inc.*

Abstract

We study multiqubit variational quantum states that can be considered as weighted quantum graph states. These states are constructed as single-layer variational circuits with RX rotations and RZZ entangling gates, corresponding to graphs of arbitrary structure. In general case of quantum graph states of arbitrary structure we derive the geometric measure of entanglement and evaluate quantum correlators. It is shown that these quantities are directly related to the degrees of the corresponding vertices in graph. As an example, we analyze the state associated with the star graph $K_{1,4}$ using noisy quantum computing on the AerSimulator. The results are in good agreement with theoretical predictions. These findings demonstrate a connection between graph structure and quantum properties, enabling the study of classical graphs via quantum computing.

Keywords: entanglement, quantum graph states, variational quantum states; quantum correlators, graph properties.

1 Introduction

Quantum computing is based on operations on multi-qubit entangled quantum states. Entanglement is widely recognized as a fundamental resource for advanced information processing tasks in quantum computing and quantum communications. It enables powerful protocols such as quantum cryptography and teleportation, and underpins the exponential speed-ups of many quantum algorithms [1, 2, 3]. Accordingly, considerable effort has been devoted to both theoretically quantifying entanglement and generating high-quality entangled states on actual devices [4]. In recent years, experiments have demonstrated genuinely multi-partite entangled states on superconducting quantum processors (e.g., entangling all 16 qubits of an IBM device and observing multi-qubit entanglement in 20-qubit systems [5, 6]). To systematically study such phenomena, researchers have proposed various measures of entanglement. In this work, we focus on the geometric measure of entanglement (GME) introduced by Shimony [7], defined as the minimum squared Fubini–Study distance between an n -qubit state and the set of all n -qubit separable (unentangled) states. This measure has an intuitive geometric meaning and, importantly, has

¹E-Mail address: khrystyna.gnatenko@gmail.com

²E-Mail address: akacz@softserveinc.com

been linked to measurable quantities in experiments. In particular, GME can be evaluated via the expectation values of spin (Pauli) operators – a relationship was shown in [8], which lays the foundation for entanglement estimation on quantum hardware [9, 10, 11].

Beyond bipartite entanglement, an ongoing research challenge is to understand how entanglement is distributed in multipartite quantum states, especially those prepared by modern parameterized quantum circuits [12, 13]. A foundational result presented in [14] revealed that highly expressive parameterized quantum circuits can suffer from barren plateaus—regions of vanishing gradients that hinder trainability—due to excessive entanglement. The authors of paper [15] introduced quantitative descriptors for expressibility and entangling capability, showing how circuit architecture and gate choices influence the ability of PQCs to generate entangled states. In [16] it was further demonstrated that the emergence of barren plateaus depends critically on the cost function and circuit depth, with local cost functions mitigating the issue in shallow circuits. Complementing these theoretical insights, authors of paper [17] empirically studied the relationship between entanglement, expressibility, and classification accuracy in PQCs, finding that while expressibility correlates with performance, entanglement alone is not always predictive of success.

One prominent family of highly entangled multipartite states are quantum graph states, which are generated by applying two-qubit entangling gates (such as controlled-phase gates) between selected pairs of qubits initialized in a product state. Graph states play a central role in quantum error correction, cryptography, and network protocols, and serve as a natural testbed for studying multi-qubit entanglement structure [18, 19]. Prior works have derived closed-form GME values for certain graph states, finding that a qubit’s entanglement is often determined by its connectedness in the interaction graph [10, 11, 20]. Recent work has also proposed variational algorithms that directly optimize over entanglement witnesses or geometric entanglement bounds, enabling scalable estimation of multipartite entanglement in noisy intermediate-scale quantum (NISQ) devices [21].

Building on prior work, we examine single-layer variational quantum states constructed using RX gates and entangling blocks composed of RZZ gates applied in an arbitrary manner. We analytically calculate both the entanglement of these states and the corresponding quantum correlators. We establish the dependence of these quantities on the classical parameters associated with the vertices of the corresponding graphs. In the specific case of star graphs, we compute the entanglement and quantum correlations using noisy quantum computing on the AerSimulator.

The paper is organised as follows. In Section 2 we calculate analytically the geometric measure of entanglement of quantum graph states and study quantum correlators in general case of graphs of arbitrary structure. In Section 4 we present results of quantum calculations of the entanglement of single-layer variational quantum states representing weighted graphs as well as and quantum computing of quantum correlators. Conclusions are presented in Section 4.

2 Properties of one-layer variational quantum states corresponding to weighted graphs

Let us study single-layer variational quantum states constructed using $RX_i(\phi_i) = \exp(-i\phi_i\sigma_i^x/2)$ gates and $RZZ_{jk}(\theta_{jk}) = \exp(-i\theta_{jk}\sigma_j^z\sigma_k^z/2)$ gates, σ_i^x , σ_i^z are Pauli matrices corresponding to qubit $q[i]$. The resulting states can be interpreted as quantum graph states. They can be represented by graphs $G(V, E)$, where the vertices V correspond to qubits and the action of two-qubit gates is represented by edges E , the weights of edges (j, k) are characterized by parameters θ_{jk} . We consider a single-layer variational quantum state that corresponds to a quantum graph state representing an arbitrary graph (with RZZ gates applied in an arbitrary manner). The state is given by:

$$|\psi_G\rangle = \prod_{(j,k)\in E} RZZ_{jk}(\theta_{jk}) \prod_i RX_i(\phi_i) |00\dots 0\rangle. \quad (1)$$

Let us study properties of the state. First we quantify the GME of one qubit $q[l]$ with others qubits in state $|\psi_I\rangle$. According to the definition [7, 8] it reads

$$E_l(|\psi_G\rangle) = \frac{1}{2} \left(1 - \sqrt{\langle\sigma^x\rangle^2 + \langle\sigma^y\rangle^2 + \langle\sigma^z\rangle^2} \right), \quad (2)$$

with $\langle\sigma_l^j\rangle = \langle\psi_I|\sigma_l^j|\psi_I\rangle^2$. The mean values for the Pauli operators read

$$\begin{aligned} \langle\sigma_l^x\rangle &= \langle 00\dots 0 | \prod_r RX_r^+(\phi_r) \prod_{j\in N_G(l)} RZZ_{jl}^+(2\theta_{jl}) \prod_p RX_p(\phi_p) \sigma_l^x | 00\dots 0 \rangle = \\ &= \sin \phi_l \Im \left[\prod_{j\in N_G(l)} \left(\cos \theta_{lj} + i \sin \theta_{lj} \cos \phi_j \right) \right]. \end{aligned} \quad (3)$$

Similarly for $\langle\sigma_l^y\rangle$ we find

$$\begin{aligned} \langle\sigma_l^y\rangle &= \langle 00\dots 0 | \prod_r RX_r^+(\phi_r) \prod_{j\in N_G(l)} RZZ_{jl}^+(2\theta_{jl}) \sigma_l^y \prod_p RX_p(\phi_p) | 00\dots 0 \rangle = \\ &= -\sin \phi_l \Re \left[\prod_{j\in N_G(l)} \left(\cos \theta_{lj} + i \sin \theta_{lj} \cos \phi_j \right) \right]. \end{aligned} \quad (4)$$

And for $\langle\sigma_l^z\rangle$ we obtain

$$\langle\sigma_l^z\rangle = \langle 00\dots 0 | \prod_r RX_r^+(\phi_r) \sigma_l^z \prod_l RX_l(\phi_l) | 0 \rangle = \cos \phi_l. \quad (5)$$

For the entanglement of qubit with other qubits in state ψ_I we have the following expression

$$E_l(|\psi_G\rangle) = \frac{1}{2} - \frac{1}{2} \sqrt{\cos^2 \phi_l + \sin^2 \phi_l \prod_{j\in N_G(l)} \left(\cos^2 \theta_{lj} + \sin^2 \theta_{lj} \cos^2 \phi_j \right)}. \quad (6)$$

In particular case, that is $\phi_i = \phi$, and $\theta_{jl} = \theta$, the results for the entanglement simplifies to the following form

$$E_l(|\psi_G\rangle) = \frac{1}{2} - \frac{1}{2} \sqrt{\cos^2 \phi + \sin^2 \phi \left(\cos^2 \theta + \sin^2 \theta \cos^2 \phi \right)^{|N_G(l)|}}, \quad (7)$$

So, the entanglement of qubit $q[l]$ with other qubits in quantum state $|\psi_I\rangle$ depends on the vertex degree $|N_G(l)|$.

Let us also calculate the correlators $\langle \psi_G | \sigma_l^\alpha \sigma_m^\beta | \psi_G \rangle = \langle \sigma_l^\alpha \sigma_m^\beta \rangle$, $\alpha, \beta = (x, y, z)$ For $\langle \sigma_l^x \sigma_m^z \rangle$ we have

$$\begin{aligned} \langle \sigma_l^x \sigma_m^z \rangle &= \langle 00\dots 0 | \prod_r R X_r^+(\phi_r) \prod_{j \in N_G(l)} R Z Z_j^+(2\theta_{jl}) \sigma_l^x \sigma_m^z \prod_p R X_p(\phi_p) | 00\dots 0 \rangle = \\ &= \sin \phi_l \cos \theta_{lm} \cos \phi_m \Im \left[\prod_{j \in N_G(l) \setminus \{m\}} \left(\cos \theta_{lj} + i \sin \theta_{lj} \cos \phi_j \right) \right] + \\ &+ \sin \phi_l \sin \theta_{lm} \Re \left[\prod_{j \in N_G(l) \setminus \{m\}} \left(\cos \theta_{lj} + i \sin \theta_{lj} \cos \phi_j \right) \right]. \end{aligned} \quad (8)$$

For $\langle \sigma_l^x \sigma_m^y \rangle$ one finds

$$\begin{aligned} \langle \sigma_l^x \sigma_m^y \rangle &= \\ &= -\sin \phi_l \sin \phi_m \left(\Im \left[\left(\cos(\theta_{lr} - \theta_{mr}) + i \sin(\theta_{lr} - \theta_{mr}) \cos \phi_r \right) \times \right. \right. \\ &\times \prod_{j \in N_G(l) \setminus \{m\}} \prod_{k \in N_G(m) \setminus \{l\}, k \neq j} \left(\cos \theta_{lj} + i \sin \theta_{lj} \cos \phi_j \right) \left(\cos \theta_{mk} - i \sin \theta_{mk} \cos \phi_j \right) + \\ &+ \left. \left(\cos(\theta_{lr} + \theta_{mr}) + i \sin(\theta_{lr} + \theta_{mr}) \cos \phi_r \right) \times \right. \\ &\times \left. \left. \prod_{j \in N_G(l) \setminus \{m\}} \prod_{k \in N_G(m) \setminus \{l\}, k \neq j} \left(\cos \theta_{lj} + i \sin \theta_{lj} \cos \phi_j \right) \left(\cos \theta_{mk} + i \sin \theta_{mk} \cos \phi_j \right) \right] \right). \end{aligned}$$

Here r is the intersection of the neighborhoods of vertices l, m in graph $G(E, V)$. Similarly for other correlators $\langle \sigma_l^\alpha \sigma_m^\beta \rangle$, $\alpha, \beta = (x, y, z)$ we find the following results

$$\begin{aligned} \langle \sigma_l^x \sigma_m^x \rangle &= \\ &= \sin \phi_l \sin \phi_m \left(\Re \left[\left(\cos(\theta_{lr} - \theta_{mr}) + i \sin(\theta_{lr} - \theta_{mr}) \cos \phi_r \right) \times \right. \right. \\ &\times \prod_{j \in N_G(l) \setminus \{m\}} \prod_{k \in N_G(m) \setminus \{l\}, k \neq j} \left(\cos \theta_{lj} + i \sin \theta_{lj} \cos \phi_j \right) \left(\cos \theta_{mk} - i \sin \theta_{mk} \cos \phi_j \right) - \\ &- \left. \left(\cos(\theta_{lr} + \theta_{mr}) + i \sin(\theta_{lr} + \theta_{mr}) \cos \phi_r \right) \times \right. \\ &\times \left. \left. \prod_{j \in N_G(l) \setminus \{m\}} \prod_{k \in N_G(m) \setminus \{l\}, k \neq j} \left(\cos \theta_{lj} + i \sin \theta_{lj} \cos \phi_j \right) \left(\cos \theta_{mk} + i \sin \theta_{mk} \cos \phi_j \right) \right] \right), \end{aligned}$$

$$\begin{aligned}
\langle \sigma_l^y \sigma_m^z \rangle &= \\
&= -\sin \phi_l \cos \theta_{lm} \cos(\phi_m) \Re \left[\prod_{j \in N_G(l) \setminus \{m\}} \left(\cos \theta_{lj} + i \sin \theta_{lj} \cos \phi_j \right) \right] + \\
&\quad + \sin \phi_l \sin \theta_{lm} \Im \left[\prod_{j \in N_G(l) \setminus \{m\}} \left(\cos \theta_{mj} + i \sin \theta_{mj} \cos \phi_j \right) \right], \tag{9}
\end{aligned}$$

$$\begin{aligned}
\langle \sigma_l^y \sigma_m^y \rangle &= \\
&= \sin \phi_l \sin \phi_m \left(\Re \left[\left(\cos(\theta_{lr} - \theta_{mr}) + i \sin(\theta_{lr} - \theta_{mr}) \cos \phi_r \right) \times \right. \right. \\
&\times \prod_{j \in N_G(l) \setminus \{m\}} \prod_{k \in N_G(m) \setminus \{l\}, k \neq j} \left(\cos \theta_{lj} + i \sin \theta_{lj} \cos \phi_j \right) \left(\cos \theta_{mk} - i \sin \theta_{mk} \cos \phi_j \right) + \\
&+ \left(\cos(\theta_{lr} + \theta_{mr}) + i \sin(\theta_{lr} + \theta_{mr}) \cos \phi_r \right) \times \\
&\times \left. \left. \prod_{j \in N_G(l) \setminus \{m\}} \prod_{k \in N_G(m) \setminus \{l\}, k \neq j} \left(\cos \theta_{lj} + i \sin \theta_{lj} \cos \phi_j \right) \left(\cos \theta_{mk} + i \sin \theta_{mk} \cos \phi_j \right) \right] \right), \\
\langle \sigma_l^z \sigma_m^z \rangle &= \cos \phi_l \cos \phi_m. \tag{10}
\end{aligned}$$

In case when all of the parameters were equal for all the qubits, that is $\phi_i = \phi$ and $\theta_{ij} = \theta$ and the intersection of the neighborhoods of vertices l, m is empty, we have relation of the quantum properties with classical ones. Namely the quantum correlators are related with the degrees of vertices $|N_G(l)|, |N_G(m)|$, representing corresponding qubits $q[l], q[m]$ in a graph. The expressions read

$$\begin{aligned}
\langle \sigma_l^x \sigma_m^z \rangle &= \sin \phi \cos \theta \cos \phi \Im \left[\left(\cos \theta + i \sin \theta \cos \phi \right)^{|N_G(l)|} \right] + \\
&\quad + \sin \phi \sin \theta \Re \left[\left(\cos \theta + i \sin \theta \cos \phi \right)^{|N_G(l)|} \right] \tag{11}
\end{aligned}$$

$$\begin{aligned}
\langle \sigma_l^x \sigma_m^y \rangle &= \\
&= -\sin(\phi) \sin(\phi) \Im \left[\left(\cos \theta + i \sin \theta \cos(\phi) \right)^{|N_G(l)|} \right] \Re \left[\left(\cos \theta + i \sin \theta \cos \phi \right)^{|N_G(m)|} \right] \tag{12}
\end{aligned}$$

$$\begin{aligned}
\langle \sigma_l^x \sigma_m^x \rangle &= \\
&= \sin \phi \sin \phi \Im \left[\left(\cos \theta + i \sin \theta \cos \phi \right)^{|N_G(l)|} \right] \Im \left[\left(\cos \theta + i \sin \theta \cos \phi \right)^{|N_G(m)|} \right] \tag{13}
\end{aligned}$$

$$\begin{aligned}
\langle \sigma_l^y \sigma_m^z \rangle &= \\
&= -\sin \phi \cos \theta \cos \phi \Re \left[\left(\cos \theta + i \sin \theta \cos \phi \right)^{|N_G(l)|} \right] + \\
&\quad + \sin \phi \sin \theta \Im \left[\left(\cos \theta + i \sin \theta \cos \phi \right)^{|N_G(l)|} \right] \tag{14}
\end{aligned}$$

So, quantifying the quantum correlators in quantum graph states one can detect these properties of graphs with quantum programming.

3 Quantum computing of the entanglement of quantum graph states and quantum correlators

Let us study properties of the quantum graph states with quantum computing. According to definition of the entanglement distance, to quantify the entanglement of qubit $q[l]$ with other qubits in the state $|\psi_G\rangle$ one need to prepare the state and measure mean values of the Pauli operators corresponding to qubit $q[l]$ in the state. The mean value of σ_l^z can be found on the basis of results of measurement of state of qubit $q[l]$ in the standard basis. To find $\langle\sigma_l^x\rangle$, $\langle\sigma_l^y\rangle$, taking into account identities $\sigma_k^x = \exp(-i\pi\sigma^y/4)\sigma_k^z \exp(i\pi\sigma^y/4)$, $\sigma_k^y = \exp(+i\pi\sigma^x/4)\sigma_k^z \exp(-i\pi\sigma^x/4)$ we have to apply the operator of rotation before the measurement in the standard basis. The mean values read $\langle\sigma_k^x\rangle = |\langle\tilde{\psi}^y|0\rangle|^2 - |\langle\tilde{\psi}^y|1\rangle|^2$, $\langle\sigma_k^y\rangle = |\langle\tilde{\psi}^x|0\rangle|^2 - |\langle\tilde{\psi}^x|1\rangle|^2$, with $|\tilde{\psi}^y\rangle = RY_k(-\pi/2)|\psi_I\rangle$, $|\tilde{\psi}^x\rangle = RX_k(\pi/2)|\psi_I\rangle$.

We calculate the geometric measure of entanglement for qubit l that is in a center of star topology graph G . The structure of the quantum circuit that encodes the example $K_{1,4}$ presented at Fig. 1.

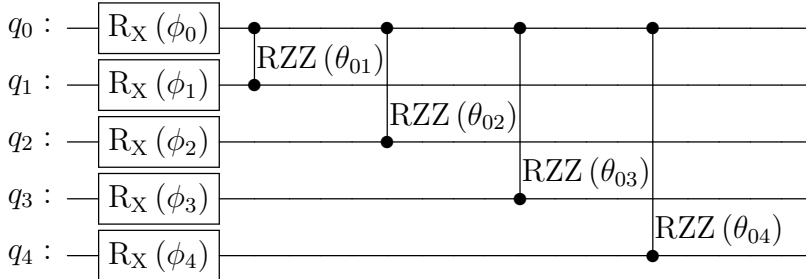


Figure 1: Quantum circuit for preparation of quantum state $|\psi_G\rangle$ corresponding to $K_{1,4}$.

Theoretical results for the spin components required to calculate the entanglement distance of qubit $q[0]$ with other qubits in quantum state $|\psi_I\rangle$ representing $K_{1,4}$ are as follows

$$\langle\sigma_0^x\rangle = \sin\phi\Im\left[\left(\cos\theta + i\sin\theta\cos\phi\right)^4\right], \quad (15)$$

$$\langle\sigma_0^y\rangle = -\sin\phi\Re\left[\left(\cos\theta + i\sin\theta\cos\phi\right)^4\right], \quad (16)$$

$$\langle\sigma_0^z\rangle = \cos\phi. \quad (17)$$

With a state-of-the-art quantum simulator, we prepare the star-graph states for various circuit parameters and compute their entanglement distance via the mean-spin method,

obtaining agreement with the derived formulas. We then emulate the state preparation on a noisy superconducting quantum device (incorporating realistic two-qubit gate errors and decoherence) to assess the robustness of the entanglement. For noisy simulation we transpiled the circuit to heavy hex lattice with basis gates set: $Id, X, SX, RZ, CNOT$ and noise model including readout error probability of 10^{-2} , X and SX gate error of order 10^{-4} and CNOT gate error of order 10^{-2} . We find that the values of the entanglement are reduced under noise – as expected – but remain in qualitative agreement with the ideal predictions. This demonstrates that the approach for evaluating entanglement with mean spin is feasible on near-term quantum processors.

We have also calculated with quantum computing on AerSimulator quantum correlators $\langle \sigma_0^\alpha \sigma_1^\beta \rangle$, $\alpha, \beta = (x, y, z)$ in quantum state $|\psi_G\rangle$, corresponding to $K_{1,4}$ (see Fig. 1). Similarly, we considered noise model including readout error probability of 10^{-2} , X and SX gate error of order 10^{-4} and CNOT gate error of order 10^{-2} . The results of quantum computing as well as absolute differences between the analytical results and results of quantum computing are presented in Figs. 3-6. The results of quantum computing are in good agreement with the theoretical ones.

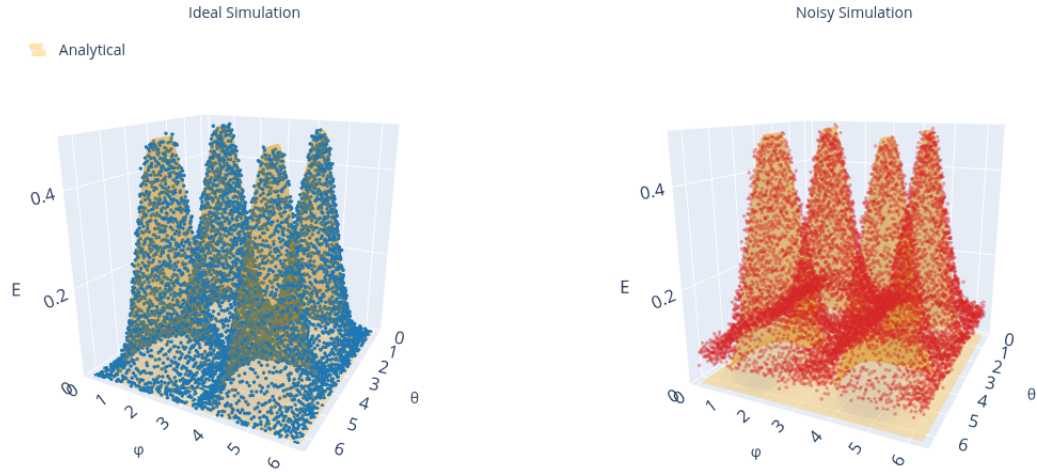


Figure 2: Surface plots of geometric measure of entanglement for quantum graph state $|\psi_G\rangle$ Fig. 1 with $\phi_i = \phi$ and $\theta_{ij} = \theta$. Yellow surface shows analytical result, blue dots were obtained from ideal simulation on AerSimulator and red dots from noisy simulation on AerSimulator with readout error probability of 10^{-2} , X and SX gate error of order 10^{-4} and CNOT gate error of order 10^{-2} .

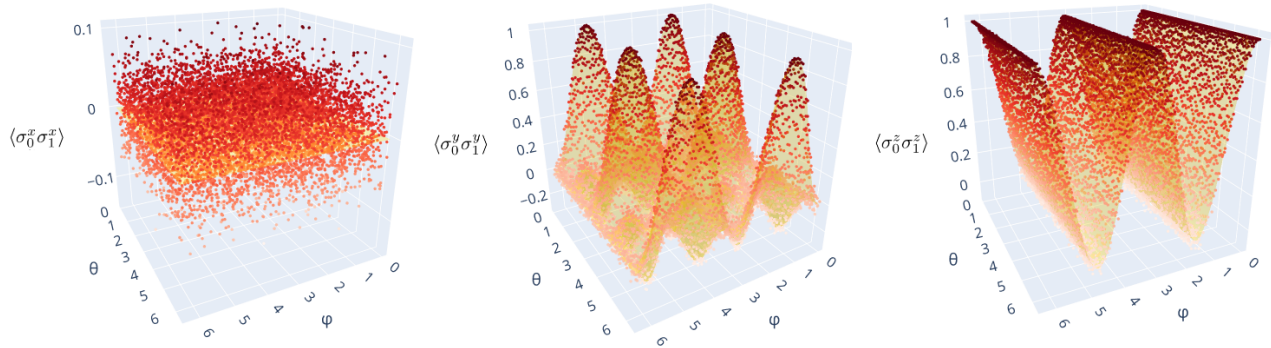


Figure 3: Surface plots of $\langle \sigma_0^x \sigma_1^x \rangle$, $\langle \sigma_0^y \sigma_1^y \rangle$, $\langle \sigma_0^z \sigma_1^z \rangle$ in quantum state $|\psi_G\rangle$ corresponding to $K_{1,4}$ graph. Surface shows analytical result, and dots are obtained from noisy quantum computing on AerSimulator

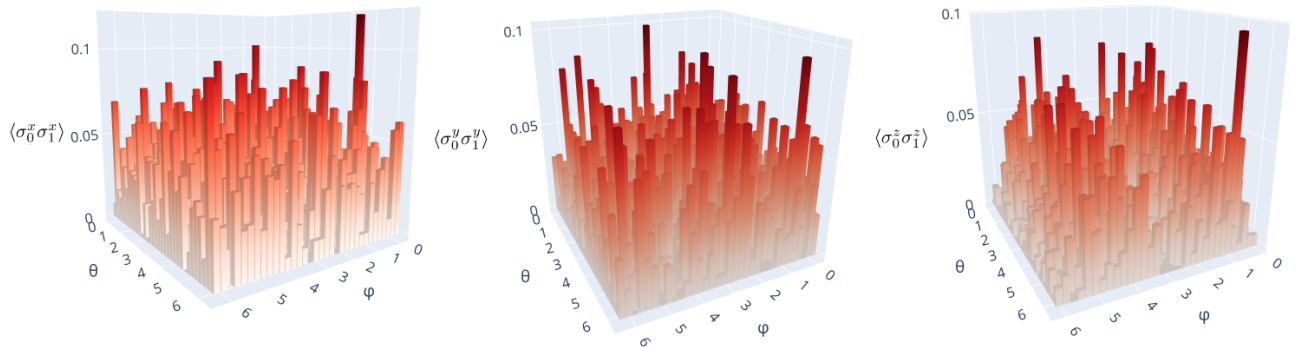


Figure 4: Bar plots of absolute differences between the analytical results for $\langle \sigma_0^x \sigma_1^x \rangle$, $\langle \sigma_0^y \sigma_1^y \rangle$, $\langle \sigma_0^z \sigma_1^z \rangle$ in quantum state $|\psi_G\rangle$ corresponding to $K_{1,4}$ graph and results of noisy quantum computing on AerSimulator.

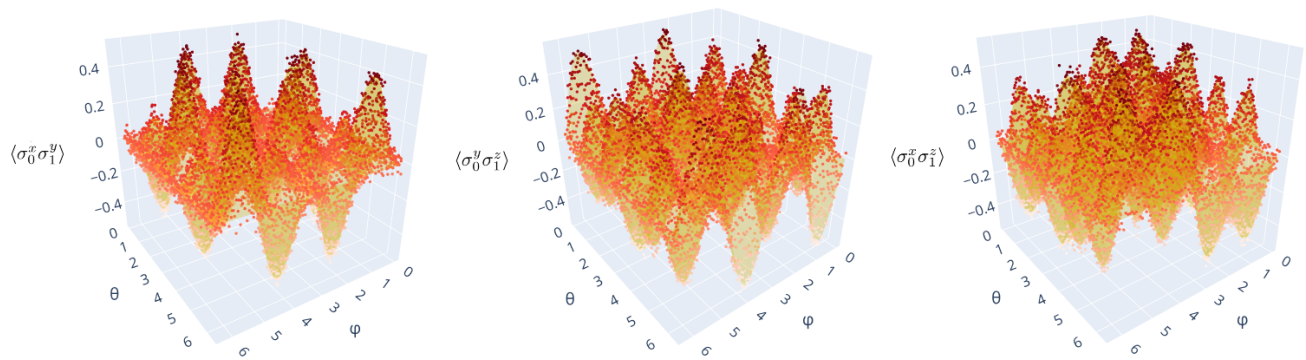


Figure 5: Surface plots of $\langle \sigma_0^x \sigma_1^y \rangle$, $\langle \sigma_0^y \sigma_1^z \rangle$, $\langle \sigma_0^x \sigma_1^z \rangle$ in quantum state $|\psi_G\rangle$ corresponding to $K_{1,4}$ graph. Surface shows analytical result, and dots are obtained from noisy quantum computing on AerSimulator

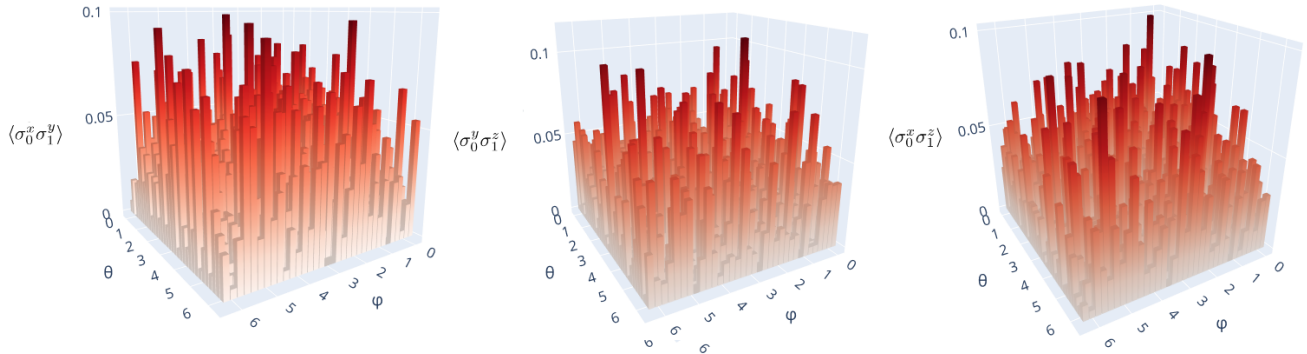


Figure 6: Bar plots of absolute differences between the analytical results for $\langle \sigma_0^x \sigma_1^y \rangle$, $\langle \sigma_0^y \sigma_1^z \rangle$, $\langle \sigma_0^x \sigma_1^z \rangle$ in quantum state $|\psi_G\rangle$ corresponding to $K_{1,4}$ graph and results of noisy quantum computing on AerSimulator.

4 Conclusions

Multiqubit quantum states that can be considered as weighted quantum graph states have been examined. The states are variational quantum states constructed with rotational blocks using RX gates and entangling blocks with RZZ gates applied in an arbitrary manner. These states correspond to weighted graphs of arbitrary structure, in which vertices are represented by qubits, edges are represented by the action of RZZ gates, and the weights of the edges are characterized by the parameters of the RZZ gates.

For these multiqubit quantum graph states representing graphs of arbitrary structure, we have obtained the geometric measure of entanglement as well as quantum correlators $\langle \sigma_l^\alpha \sigma_m^\beta \rangle$, where $\alpha, \beta = (x, y, z)$. It was found that these quantum quantities depend on the classical properties of the vertices in the corresponding graphs. Namely, the entanglement of qubit $q[l]$ in the quantum graph state is related to the degree of the corresponding vertex in the graph, while the correlators $\langle \sigma_l^\alpha \sigma_m^\beta \rangle$ depend on the degrees of vertices l and m .

The obtained results are fundamental, because the properties of multi-qubit states are important resources for quantum computing. Moreover, these results open up the possibility of studying properties of classical objects such as graphs using quantum computing.

In the particular case of a quantum state corresponding to the graph $K_{1,4}$, we have studied the entanglement as well as quantum correlators using quantum computing on the AerSimulator. The effect of noise on the results of quantum calculations was also examined. The results of quantum simulations are in good agreement with the theoretical predictions.

References

- [1] A. K. Ekert, “Quantum cryptography based on bell’s theorem,” *Phys. Rev. Lett.*, vol. 67, pp. 661–663, Aug 1991.

- [2] C. H. Bennett, G. Brassard, C. Crépeau, R. Jozsa, A. Peres, and W. K. Wootters, “Teleporting an unknown quantum state via dual classical and einstein-podolsky-rosen channels,” *Phys. Rev. Lett.*, vol. 70, pp. 1895–1899, Mar 1993.
- [3] R. Jozsa and N. Linden, “On the role of entanglement in quantum-computational speed-up,” *Proceedings of the Royal Society A: Mathematical, Physical and Engineering Sciences*, vol. 459, pp. 2011–2032, 08 2003.
- [4] R. Horodecki, P. Horodecki, M. Horodecki, and K. Horodecki, “Quantum entanglement,” *Rev. Mod. Phys.*, vol. 81, pp. 865–942, Jun 2009.
- [5] Y. Wang, Y. Li, Z.-q. Yin, and B. Zeng, “16-qubit ibm universal quantum computer can be fully entangled,” *npj Quantum Information*, vol. 4, p. 46, Sep 2018.
- [6] N. Friis, O. Marty, C. Maier, C. Hempel, M. Holzäpfel, P. Jurcevic, M. B. Plenio, M. Huber, C. Roos, R. Blatt, and B. Lanyon, “Observation of entangled states of a fully controlled 20-qubit system,” *Phys. Rev. X*, vol. 8, p. 021012, Apr 2018.
- [7] A. Shimony, “Degree of entanglement,” *Annals of the New York Academy of Sciences*, vol. 755, pp. 675–679, 1995.
- [8] A. Frydryszak, M. I. Samar, and V. M. Tkachuk, “Quantifying geometric measure of entanglement by mean value of spin and spin correlations with application to physical systems,” *European Physical Journal D*, vol. 71, p. 233, 2017.
- [9] A. Kuzmak and V. Tkachuk, “Detecting entanglement by the mean value of spin on a quantum computer,” *Physics Letters A*, vol. 384, p. 126579, Aug. 2020.
- [10] K. P. Gnatenko and N. A. Susulovska, “Geometric measure of entanglement of multi-qubit graph states and its detection on a quantum computer,” *Europhysics Letters*, vol. 136, p. 40003, Nov. 2021.
- [11] K. Gnatenko, “Entanglement of multi-qubit states representing directed networks and its detection with quantum computing,” *Physics Letters A*, vol. 521, p. 129815, Oct. 2024.
- [12] O. Gühne and G. Tóth, “Entanglement detection,” *Physics Reports*, vol. 474, no. 1, pp. 1–75, 2009.
- [13] A. Vesperini, “Multipartite entanglement and geometry of quantum states,” *Annals of Physics*, vol. 457, p. 169406, 2023.
- [14] J. R. McClean, S. Boixo, V. N. Smelyanskiy, R. Babbush, and H. Neven, “Barren plateaus in quantum neural network training landscapes,” *Nature Communications*, vol. 9, no. 1, p. 4812, 2018.
- [15] S. Sim, P. D. Johnson, and A. Aspuru-Guzik, “Expressibility and entangling capability of parameterized quantum circuits for hybrid quantum-classical algorithms,” *Advanced Quantum Technologies*, vol. 2, no. 12, p. 1900070, 2019.
- [16] M. Cerezo, A. Sone, T. Volkoff, L. Cincio, and P. J. Coles, “Cost function dependent barren plateaus in shallow parametrized quantum circuits,” *Nature Communications*, vol. 12, no. 1, p. 1791, 2021.

- [17] T. Hubregtsen, J. Pichlmeier, P. Stecher, and K. Bertels, “Evaluation of parameterized quantum circuits: on the relation between classification accuracy, expressibility, and entangling capability,” *Quantum Machine Intelligence*, vol. 3, no. 9, 2021.
- [18] R. Raussendorf and H. J. Briegel, “A one-way quantum computer,” *Phys. Rev. Lett.*, vol. 86, pp. 5188–5191, May 2001.
- [19] D. Markham and B. C. Sanders, “Graph states for quantum secret sharing,” *Phys. Rev. A*, vol. 78, p. 042309, Oct 2008.
- [20] K. P. Gnatenko, “Evaluation of variational quantum states entanglement on a quantum computer by the mean value of spin,” 2023.
- [21] V. Azimi-Mousolou and P. Singh, “Variational m-partite geometric entanglement algorithm,” *arXiv preprint arXiv:2503.20056*, 2025.